Hindawi
Mathematical Problems in Engineering
Volume 2022, Article ID 7218213, 11 pages
https://doi.org/10.1155/2022/7218213

Research Article

Overlapping Decentralized Guaranteed Cost Control Method for Discrete-Time Systems of Building Structures with Uncertain Parameters under Earthquake Action

Qinghu Xu,[1,2,3] Yu Zhang,[1] Xuezhi Zhen,[1] Dawei Man,[1,2,3] Xiaofang Kang,[1,2,3] Guanghui Xia,[1,2,3] and Xianzeng Shi[1,4]

[1]*School of Civil Engineering, Anhui Jianzhu University, Hefei 230601, China*
[2]*BIM Engineering Center of Anhui Province, Hefei 230601, China*
[3]*Prefabricated Building Research Institute of Anhui Province, Hefei 230601, China*
[4]*College of Civil and Transportation Engineering, Hohai University, Nanjing 210098, China*

Correspondence should be addressed to Dawei Man; mandawei@ahjzu.edu.cn

Received 31 March 2022; Accepted 25 April 2022; Published 28 May 2022

Academic Editor: Alfrendo Satyanaga

This paper proposes a discrete-time overlapping decentralized guaranteed cost control algorithm via state feedback. Based on the inclusion principle, a structure system is decoupled into multiple subsystems, and the discretized subsystems' controllers are designed by using the guaranteed cost control algorithm. Finally, the subsystems' controllers are contracted into overlapping controllers of the original system, and the design of the control system is completed. This control method is introduced to the civil engineering field to solve the seismic control problem for discrete-time systems of building structures with uncertain parameters. The numerical analysis of the nine-story building structure model with uncertain parameters is carried out. The results show that the proposed control method can still effectively reduce the seismic response of discrete-time system when the structural parameters are uncertain, and the control effect is similar to the centralized control strategy; at the same time, the sampling rate and data transmission speed of the system are improved to ensure the reliability of the system. It illustrates the feasibility and effectiveness of the presented approach.

1. Introduction

The problem of real-time feedback control of control systems has been in focus for a long time [1–3]. A complete structural vibration control system generally consists of actuators, controllers, and sensors. The performance of the control system is determined by the real-time and accurate information transfer between these devices. The use of wireless transmission technology to replace traditional cable transmission can effectively improve the real-time performance of system information transmission and reduce the cost of control system [4]. The emergence of advanced technologies, such as the wireless networked control systems (WNCS), digital computers, and micro controllers, promotes the popularization and application of control system in practical engineering [5, 6]. The corresponding control force can be calculated in real time through the feedback information of each sampling, which is then converted into an analog signal in the form of a step function that is applied to the structure in the real-time feedback control system. In essence, the measurement information and input control force in the system are discrete-time, rather than the continuous-time function required by the continuous-time control algorithm [7]. The control algorithm designed by discrete-time method is more in line with the actual situation of the controlled system. Therefore, it is particularly necessary to study the structural vibration control of discrete-time systems. Paul et al. [8] proposed a novel discrete-time sliding mode control in order to attenuate the bidirectional vibrations of building structures, comparing the fuzzy sliding mode control with conventional controllers, which was found to be the most effective in mitigating bidirectional and torsional vibrations. Kemerli et al. [9] proposed the design and implementation of the discrete-time sliding mode controller with a hybrid control strategy according to Gao's reaching law and variable rate reaching law and conducted simulated experiments with a 5-story building under seismic excitation; the results show that better results were achieved in terms of controller energy consumption and structural response compared to Gao's controller. Demir et al. [10] studied a method to stabilize the static output feedback (SOF) of a discrete-time linear time-invariant (LTI) system by using a small number of sensors. Gómez et al. [11] discussed the active control of building structures subjected to tridirectional earthquake excitation, for which there is no available mathematical model, the discrete-time hysteretic nonlinear model was developed, and use the pole-placement design to control the building structure in bidirectional with vertical and torsional effects. They performed a two-story building prototype to verify that the controller worked better than other horizontal and torsional actuators. The centralized control strategies are mostly used to suppress the vibration response of multi-degree-of-freedom structures in previous studies. Although it can obtain good control effects, there are also disadvantages such as long feedback time and poor stability of the system. Therefore, the decentralized control strategy is with the advantages of fast data transmission and less feedback delay and strong system reliability received extensive attention from researchers [12–15]. Liu et al. [16] proposed decentralized state feedback control based on substructure (S-DSFC) algorithm. A numerical study of a 6-story plane frame under seismic excitation indicated that both the substructure and the whole structural system could have better control and stability compared with the traditional decentralized control method. Fadhilah et al. [17] used the information from its own subsystem and other subsystems based on the interconnection to design decentralized controllers. The bilinear matrix inequality (BMI) problem is solved by the homotopy method, and the decentralized controller is found to have better attenuation of centralized disturbances compared to the state feedback controller by two numerical example simulations. Palacios-Quiñonero et al. [18] introduced a high-performance decentralized controller for vibration control of large building structures. A 35-story building is used as a research object to verify the flexibility and effectiveness of the decentralized control strategy. Experimental results show that the controller remains structured despite severe integration constraints. Aboudonia et al. [19] proposed a passive-based control scheme for discrete-time systems in which the control synthesis and operation are decentralized. The study chose appropriately cost functions for control, resulting in controllers that may lead to closed-loop behavior similar to LQR, then considering local conditions to ensure local passivity of all subsystems which implies asymptotic stability of the whole system. Zhu et al. [20] developed a control method of decentralized predictor based on large-scale systems with large input delay, and two methods for the delay compensation were proposed: the backstepping-based partial differential equation (PDE) approach and the reduction-based ordinary differential equation (ODE) approach. Then, the Lyapunov-based dispersion analysis is proposed under the two prediction methods. The proposed methods are shown to be effective through two benchmark examples of coupled cart-pendulum systems when the input delay of the stabilization system is too large without predictor. Warsewa et al. [21] proposed a method for designing decentralized and distributed observers that can be used for the monitoring and control of large-scale adaptive structures. In scenarios where redundancy and decentralization are important, it provides a valuable approach for designing new types of observers for intelligent structures.

However, the above literature did not consider the existence of parameter uncertainty in the structural system when studying the system vibration control problem. This uncertainty can have a negative impact on the performance of the controlled system, so the influence of this uncertainty needs to be considered in the design of the controller. The guaranteed cost control algorithm provides an effective way to solve this class of control problems, and the method allows a defined upper bound on the performance index of the system while also ensuring its robust stability [22]. Zhang et al. [23] studied the guaranteed cost control problem for a kind of nonlinear discrete-time-delay system. A complete Lyapunov-Krasovskii function was constructed based on the Lyapunov matrix. The usefulness of the theoretical results is illustrated by presenting an example. Chen et al. [24] paid attention to the guaranteed cost control problem for a class of fractional-order (FO) uncertain linear systems with time-delay parameter uncertainties with norm-bounded. By using the linear matrix inequality (LMI) method and FO Razumikhin theorem, two design methods of guaranteed cost controllers with independent time delay and their guaranteed cost are given. Two numerical examples are studied to verify the effectiveness of theoretical formulas. Qi et al. [25] also studied the guaranteed cost control problem for a class of uncertain fractional-order (FO) linear systems with time-delay parameter uncertainties with norm-bounded by the linear matrix inequality (LMI) method and the FO Razumikhin theorem. Aiming at the admissible uncertainty, a time-delay and order-dependent design method with guaranteed closed-loop stability and cost are proposed. Chen et al. [26] analyzed the main influencing factors of the higher-order CSI effect. These include the input frequency of the control voltage, the uncertainty of the structural parameters, and the control gain. In addition, a new time-delay compensation controller based on the guaranteed cost control (GCC) algorithm is proposed to consider multilevel higher-order CSI effects. Li et al. [27] proposed a state feedback controller based on guaranteed cost control (GCC) algorithm according to a Lyapunov stability theory and linear matrix inequality (LMI) method. A ten-story frame with AMD system is analyzed. The results show that the new controller can effectively suppress the dynamic response of high-rise buildings with parameter uncertainty.

The paper studies the discrete-time system with uncertain parameters and proposes the overlapping decentralized guaranteed cost control algorithm based on state feedback. Taking a 9-story building structure under earthquake action as the research object, firstly, the guaranteed cost control equations in the discrete-time domain are derived considering the existence of uncertainties in the parameters of mass, damping, and stiffness of the structural system [27, 28]. The system is extended and decoupled using the inclusion principle and then discretized, and subcontrollers are designed with guaranteed cost control algorithms. Finally, the contraction principle is applied to form the overlapping controller of the original system. The numerical analysis results show that the control method proposed in this paper can suppress the dynamic response of the structure well, and its control effect is comparable to that of the traditional centralized control strategy, which illustrates its effectiveness.

2. Mechanical Model of Building Structure with Uncertain Parameters

Considering the uncertainties of the mass, damping, stiffness, and other parameters of the building structure system, the motion equation of the structure under seismic excitation is obtained:

$$(\mathbf{M}+\Delta\mathbf{M})\ddot{x}(t)+(\mathbf{C}+\Delta\mathbf{C})\dot{x}(t)+(\mathbf{K}+\Delta\mathbf{K})\mathbf{x}(t)=\mathbf{D}_s\ddot{x}_g(t)+\mathbf{B}_u\mathbf{u}(t), \tag{1}$$

where $\mathbf{M}$, $\Delta\mathbf{M}$ represent the mass matrix and variation matrix of the structure, respectively; $\mathbf{C}$, $\Delta\mathbf{C}$ represent the damping matrix and variation matrix of the structure, respectively; $\mathbf{K}$, $\Delta\mathbf{K}$ represent the stiffness matrix and variation matrix of the structure, respectively; $\mathbf{x}$, $\dot{x}$, $\ddot{x}$ represent the displacement, velocity, and acceleration vectors, respectively; $\mathbf{D}_s$, $\mathbf{B}_u$ represent the position matrices of the external excitation and actuator, respectively; $\ddot{x}_g$ represents the external excitation vector; and u represents the actuator control force vector.

The structural form of the corresponding parameters in (1) is

$$\begin{aligned}
\mathbf{M} &= \mathrm{diag}\{m_1, m_2, \ldots, m_n\},\\
\mathbf{C} &= \begin{bmatrix} c_1+c_2 & -c_2 & & & & \\ -c_2 & c_2+c_3 & -c_3 & & & \\ & -c_3 & c_3+c_4 & -c_4 & & \\ & & \cdots & \cdots & \cdots & \\ & & & -c_{n-1} & c_{n-1}+c_n & -c_n \\ & & & & -c_n & c_n \end{bmatrix},\\
\mathbf{K} &= \begin{bmatrix} k_1+k_2 & -k_2 & & & & \\ -k_2 & k_2+k_3 & -k_3 & & & \\ & -k_3 & k_3+k_4 & -k_4 & & \\ & & \cdots & \cdots & \cdots & \\ & & & -k_{n-1} & k_{n-1}+k_n & -k_n \\ & & & & -k_n & k_n \end{bmatrix},\\
\mathbf{D}_s &= -(\mathbf{M}+\Delta\mathbf{M})[\mathbf{1}]_{n\times 1},\\
\mathbf{B}_u &= \begin{cases} (B_u)_{i,i}=1, & 1\le i\le n,\\ (B_u)_{i,i+1}=-1, & 1\le i<n,\\ (B_u)_{i,j}=0, & \text{else,}\end{cases}\\
\Delta\mathbf{M} &= \alpha\boldsymbol{\delta}_{\mathbf{M}}\mathbf{M},\\
\Delta\mathbf{C} &= \beta\boldsymbol{\delta}_{\mathbf{C}}\mathbf{C},\\
\Delta\mathbf{K} &= \gamma\boldsymbol{\delta}_{\mathbf{K}}\mathbf{K},
\end{aligned} \tag{2}$$

where α, β, γ represent the rate of change of the mass, damping, and stiffness; and $\delta_{\mathbf{M}}$, $\delta_{\mathbf{C}}$, $\delta_{\mathbf{K}}$ are the unknown matrices of corresponding dimension. From the literature [29], we can obtain

$$\begin{aligned}
(\mathbf{M}+\Delta\mathbf{M})^{-1} &= \mathbf{M}^{-1}+\Delta_1\mathbf{M},\\
\Delta_1\mathbf{M} &= -\left(\alpha\mathbf{M}^{-1}\right)\boldsymbol{\delta}_M\left(\mathbf{I}+\alpha\boldsymbol{\delta}_{\mathbf{M}}\right)^{-1}.
\end{aligned} \tag{3}$$

The state-space model is transformed by (1):

$$\dot{Z}_p(t)=\left(\mathbf{A}_p+\Delta\mathbf{A}_p\right)\mathbf{Z}_p(t)+\left(\mathbf{B}_p+\Delta\mathbf{B}_p\right)\mathbf{u}(t)+\mathbf{E}_p\ddot{x}_g(t), \tag{4}$$

where

$$\begin{aligned}
\mathbf{A}_p &= \begin{bmatrix} \mathbf{0} & \mathbf{I} \\ -\mathbf{M}^{-1}\mathbf{K} & -\mathbf{M}^{-1}\mathbf{C} \end{bmatrix},\\
\mathbf{B}_p &= \begin{bmatrix} \mathbf{0} \\ \mathbf{M}^{-1}\mathbf{B}_u \end{bmatrix},\\
\mathbf{E}_p &= \begin{bmatrix} \mathbf{0} \\ -[\mathbf{1}] \end{bmatrix},\\
\mathbf{Z}_p(t) &= \begin{bmatrix} \mathbf{x} \\ \dot{\mathbf{x}} \end{bmatrix},\\
\Delta\mathbf{A}_p &= \begin{bmatrix} \mathbf{0} & \mathbf{0} \\ -\Delta_{\mathbf{MK}} & -\Delta_{\mathbf{MC}} \end{bmatrix},\\
\Delta\mathbf{B}_p &= \begin{bmatrix} \mathbf{0} \\ \Delta_1\mathbf{M}\mathbf{B}_u \end{bmatrix},\\
\Delta_{\mathbf{MK}} &= \Delta_1\mathbf{M}(\mathbf{K}+\Delta\mathbf{K})+\mathbf{M}^{-1}\Delta\mathbf{K},\\
\Delta_{\mathbf{MC}} &= \Delta_1\mathbf{M}(\mathbf{C}+\Delta\mathbf{C})+\mathbf{M}^{-1}\Delta\mathbf{C},\\
\begin{pmatrix}\Delta\mathbf{A}_p & \Delta\mathbf{B}_p\end{pmatrix} &= \mathbf{D}_p\mathbf{F}_p\begin{pmatrix}\mathbf{E}_{p1} & \mathbf{E}_{p2}\end{pmatrix}.
\end{aligned} \tag{5}$$

We define a new state vector:

$$\mathbf{Z}(t)=\overline{T}\mathbf{Z}_p(t). \tag{6}$$

The transformation matrix [22] $\overline{T}$ can be expressed as follows:

$$\overline{T} = \begin{cases} \overline{T}_{1,1} = 1, \\ \overline{T}_{2,n+1} = 1, \\ \overline{T}_{2i-1,i-1} = -1, \overline{T}_{2i-1,i} = 1, & 1 < i \leq n, \\ \overline{T}_{2i,n+i-1} = -1, \overline{T}_{2i,n+i} = 1, & 1 < i \leq n, \\ \overline{T}_{i,j} = 0, & \text{else}. \end{cases} \quad (7)$$

The equation of state after conversion can be expressed as

$$\dot{Z}(t) = (\mathbf{A} + \Delta\mathbf{A})\mathbf{Z}(t) + (\mathbf{B} + \Delta\mathbf{B})\mathbf{u}(t) + \mathbf{E}\ddot{x}_g(t), \quad (8)$$

where

$$\begin{aligned} \mathbf{A} &= \overline{T}\mathbf{A}_p\overline{T}^{-1}, \\ \mathbf{B} &= \overline{T}\mathbf{B}_p, \\ \mathbf{E} &= \overline{T}\mathbf{E}_p, \\ \Delta\mathbf{A} &= \overline{T}\Delta\mathbf{A}_p\overline{T}^{-1}, \\ \Delta\mathbf{B} &= \overline{T}\Delta\mathbf{B}_p. \end{aligned} \quad (9)$$

3. Guaranteed Cost Control Method for Discrete-Time Systems

Taking the sampling period $\Delta T = 0.02s$, the continuous-time system (8) is discretized to obtain the state-space model of the discrete-time system,

$$\mathbf{Z}(k+1) = (\mathbf{A} + \Delta\mathbf{A})\mathbf{Z}(k) + (\mathbf{B} + \Delta\mathbf{B})\mathbf{u}(k) + \mathbf{E}\ddot{x}_g(k), \quad (10)$$

where $\mathbf{A}$, $\mathbf{B}$ are constant matrices, and $\Delta\mathbf{A}, \Delta\mathbf{B}$ are its corresponding unknown matrices; $\mathbf{Z}(k) \in \mathbf{R}^n$ represents the state vector of the system; and $\mathbf{u}(k) \in \mathbf{R}^m$ represents the control vector of the system. It is assumed that the uncertain matrices can be expressed as follows:

$$[\Delta\mathbf{A} \;\; \Delta\mathbf{B}] = \mathbf{D}\mathbf{F}[\mathbf{E}_1 \;\; \mathbf{E}_2], \quad (11)$$

where $\mathbf{D}$, $\mathbf{E}_1$, $\mathbf{E}_2$ represent the matrices of known constants with uncertain information. $\mathbf{F} \in \mathbf{R}^{i\times j}$ is the unknown matrix satisfying the following condition:

$$\mathbf{F}^{\mathrm{T}}\mathbf{F} \leq \mathbf{I}, \quad (12)$$

and it can be time-varying.

A performance indicator is defined for system (10):

$$J = \sum_{k=0}^{\infty} \mathbf{Z}^{\mathrm{T}}(k)\mathbf{Q}^*\mathbf{Z}(k) + \mathbf{u}^{\mathrm{T}}(k)\mathbf{R}^*\mathbf{u}(k), \quad (13)$$

where $\mathbf{Q}^*, \mathbf{R}^*$ are the given symmetric positive definite weighting matrices.

Definition 1. For system (10) and the performance index (13), if there is a matrix $\mathbf{G}$ and a positive definite symmetric matrix $\mathbf{P}$ such that for all nonzero $\mathbf{Z}(k)$ and all uncertain matrices satisfying equation (12), we have

$$\begin{aligned} &\mathbf{Z}^{\mathrm{T}}(k)[\mathbf{A} + \mathbf{B}\mathbf{G} + \mathbf{D}\mathbf{F}(\mathbf{E}_1 + \mathbf{E}_2\mathbf{G})]^{\mathrm{T}}\mathbf{P}[\mathbf{A} + \mathbf{B}\mathbf{G} + \mathbf{D}\mathbf{F}(\mathbf{E}_1 + \mathbf{E}_2\mathbf{G})]\mathbf{Z}(k) \\ &\quad -\mathbf{Z}^{\mathrm{T}}(k)\mathbf{P}\mathbf{Z}(k) + \mathbf{Z}^{\mathrm{T}}(k)\left(\mathbf{Q}^* + \mathbf{G}^{\mathrm{T}}\mathbf{R}^*\mathbf{G}\right)\mathbf{Z}(k) < \mathbf{0}. \end{aligned} \quad (14)$$

The control law $\mathbf{u}(k) = \mathbf{G}\mathbf{Z}(k)$ is called a quadratic guaranteed cost control law with a performance matrix $\mathbf{P}$ for system (10).

Lemma 1 (see[30]). *It is assumed that $\mathbf{Y}_c$, $\mathbf{D}_c$, $\mathbf{E}_c$ are the known matrices and $\mathbf{Y}_c$ is symmetric, then*

$$\mathbf{Y}_c + \mathbf{D}_c\mathbf{F}\mathbf{E}_c + \mathbf{E}_c^{\mathrm{T}}\mathbf{F}^{\mathrm{T}}\mathbf{D}_c^{\mathrm{T}} < 0. \quad (15)$$

For all uncertain matrices $\mathbf{F}$ satisfying $\mathbf{F}^{\mathrm{T}}\mathbf{F} \leq \mathbf{I}$, if and only if there exists a constant $\varepsilon > 0$, such that

$$\mathbf{Y}_c + \varepsilon\mathbf{D}_c\mathbf{D}_c^{\mathrm{T}} + \varepsilon^{-1}\mathbf{E}_c^{\mathrm{T}}\mathbf{E}_c < 0. \quad (16)$$

Theorem 1 (see[31]). *If $\mathbf{u}(k) = \mathbf{G}\mathbf{Z}(k)$ is a guaranteed cost control law with performance matrix $\mathbf{P}$ for system (10) and performance index (13), then the closed-loop system*

$$\mathbf{Z}(k+1) = [\mathbf{A} + \mathbf{B}\mathbf{G} + \mathbf{D}\mathbf{F}(\mathbf{E}_1 + \mathbf{E}_2\mathbf{G})]\mathbf{Z}(k), \quad (17)$$

which is quadratically stable for all allowed uncertainties and the corresponding closed-loop performance index values satisfy the following form:

$$J \leq \mathbf{Z}_0^{\mathrm{T}}\mathbf{P}\mathbf{Z}_0. \quad (18)$$

Theorem 2 (see[31]). *For system (10) and performance index (13), if the following optimization problem*

$$\begin{aligned} &\min_{\varepsilon,X,W,Y} \operatorname{Trace}(\mathbf{W}), \\ &\text{s.t. (i)} \begin{bmatrix} \varepsilon\mathbf{D}\mathbf{D}^{\mathrm{T}} - \mathbf{X} & \mathbf{A}\mathbf{X} + \mathbf{B}\mathbf{Y} & \mathbf{0} & \mathbf{0} & \mathbf{0} \\ (\mathbf{A}\mathbf{X} + \mathbf{B}\mathbf{Y})^{\mathrm{T}} & -\mathbf{X} & (\mathbf{E}_1\mathbf{X} + \mathbf{E}_2\mathbf{Y})^{\mathrm{T}} & \mathbf{X} & \mathbf{Y}^{\mathrm{T}} \\ \mathbf{0} & \mathbf{E}_1\mathbf{X} + \mathbf{E}_2\mathbf{Y} & -\varepsilon\mathbf{I} & \mathbf{0} & \mathbf{0} \\ \mathbf{0} & \mathbf{X} & \mathbf{0} & -(\mathbf{Q}^*)^{-1} & \mathbf{0} \\ \mathbf{0} & \mathbf{Y} & \mathbf{0} & \mathbf{0} & -(\mathbf{R}^*)^{-1} \end{bmatrix} < \mathbf{0} \\ &\text{(ii)} \begin{bmatrix} \mathbf{X} & \mathbf{I} \\ \mathbf{I} & \mathbf{W} \end{bmatrix} > \mathbf{0}, \end{aligned} \quad (19)$$

which have an optimal solution $(\varepsilon_{opt}, \mathbf{Y}_{opt}, \mathbf{X}_{opt}, \mathbf{W}_{opt})$, then $\mathbf{u}(k) = \mathbf{Y}_{opt}\mathbf{X}_{opt}^{-1}\mathbf{Z}(k)$ is the optimal quadratic guaranteed cost control law of system (10), and the corresponding upper bound of system performance is $J^* = Trace(\mathbf{X}_{opt}^{-1})$.

Proof. According to Definition 1, there exists a quadratic guaranteed cost control law $\mathbf{u}(k) = \mathbf{G}\mathbf{Z}(k)$ for system (10). A matrix inequality holds if and only if there exists a matrix $\mathbf{G}$ and a symmetric matrix $\mathbf{P} > 0$ such that for the allowed uncertain matrix $\mathbf{F}$, the following matrix inequality holds:

$$\begin{aligned} &[\mathbf{A} + \mathbf{B}\mathbf{G} + \mathbf{D}\mathbf{F}(\mathbf{E}_1 + \mathbf{E}_2\mathbf{G})]^{\mathrm{T}}\mathbf{P}[\mathbf{A} + \mathbf{B}\mathbf{G} + \mathbf{D}\mathbf{F}(\mathbf{E}_1 + \mathbf{E}_2\mathbf{G})] \\ &\quad - \mathbf{P} + \mathbf{Q}^* + \mathbf{G}^{\mathrm{T}}\mathbf{R}^*\mathbf{G} < \mathbf{0}. \end{aligned} \quad (20)$$

By the Schur complementary property of matrices, (20) can be equated to

$$\begin{bmatrix} -\mathbf{P}^{-1} & [\mathbf{A}+\mathbf{BG}+\mathbf{DF}(\mathbf{E}_1+\mathbf{E}_2\mathbf{G})] \\ [\mathbf{A}+\mathbf{BG}+\mathbf{DF}(\mathbf{E}_1+\mathbf{E}_2\mathbf{G})]^{\mathrm{T}} & -\mathbf{P}+\mathbf{Q}^*+\mathbf{G}^{\mathrm{T}}\mathbf{R}^*\mathbf{G} \end{bmatrix} < \mathbf{0}. \tag{21}$$

We define the matrix

$$\Pi = \begin{bmatrix} -\mathbf{P}^{-1} & \mathbf{A}+\mathbf{BG} \\ (\mathbf{A}+\mathbf{BG})^{\mathrm{T}} & -\mathbf{P}+\mathbf{Q}^*+\mathbf{G}^{\mathrm{T}}\mathbf{R}^*\mathbf{G} \end{bmatrix}. \tag{22}$$

We convert (21) to

$$\Pi + \begin{bmatrix} \mathbf{D} \\ \mathbf{0} \end{bmatrix}\mathbf{F}[\,\mathbf{0}\ \ (\mathbf{E}_1+\mathbf{E}_2\mathbf{G})\,] + [\,\mathbf{0}\ \ (\mathbf{E}_1+\mathbf{E}_2\mathbf{G})\,]^{\mathrm{T}}\mathbf{F}^{\mathrm{T}}\begin{bmatrix} \mathbf{D} \\ \mathbf{0} \end{bmatrix}^{\mathrm{T}} < \mathbf{0}. \tag{23}$$

According to Lemma 1, the matrix inequality (23) holds for all matrices $\mathbf{F}$ that satisfy $\mathbf{F}^{\mathrm{T}}\mathbf{F} \le \mathbf{I}$. If and only if there exists a constant $\varepsilon > 0$ such that

$$\Pi + \varepsilon\begin{bmatrix} \mathbf{D} \\ \mathbf{0} \end{bmatrix}[\,\mathbf{D}^{\mathrm{T}}\ \ \mathbf{0}\,] + \varepsilon^{-1}\begin{bmatrix} \mathbf{0} \\ (\mathbf{E}_1+\mathbf{E}_2\mathbf{G})^{\mathrm{T}} \end{bmatrix}[\,\mathbf{0}\ \ (\mathbf{E}_1+\mathbf{E}_2\mathbf{G})\,] < \mathbf{0}, \tag{24}$$

then

$$\begin{bmatrix} \varepsilon\mathbf{D}\mathbf{D}^{\mathrm{T}}-\mathbf{P}^{-1} & \mathbf{A}+\mathbf{BG} \\ (\mathbf{A}+\mathbf{BG})^{\mathrm{T}} & -\mathbf{P}+\mathbf{Q}^*+\mathbf{G}^{\mathrm{T}}\mathbf{R}^*\mathbf{G}+\varepsilon^{-1}(\mathbf{E}_1+\mathbf{E}_2\mathbf{G})^{\mathrm{T}}(\mathbf{E}_1+\mathbf{E}_2\mathbf{G}) \end{bmatrix} < \mathbf{0}. \tag{25}$$

Multiplying the matrix on the left side of the above equation left and right by the matrix,

$$\begin{bmatrix} \mathbf{I} & \mathbf{0} \\ \mathbf{0} & \mathbf{P}^{-1} \end{bmatrix}, \tag{26}$$

respectively. We can obtain

$$\begin{bmatrix} \varepsilon\mathbf{D}\mathbf{D}^{\mathrm{T}}-\mathbf{P}^{-1} & (\mathbf{A}+\mathbf{BG})\mathbf{P}^{-1} \\ \mathbf{P}^{-1}(\mathbf{A}+\mathbf{BG})^{\mathrm{T}} & -\mathbf{P}^{-1}+\mathbf{P}^{-1}\left(\mathbf{Q}^*+\mathbf{G}^{\mathrm{T}}\mathbf{R}^*\mathbf{G}\right)\mathbf{P}^{-1}+\mathbf{P}^{-1}\left[\varepsilon^{-1}(\mathbf{E}_1+\mathbf{E}_2\mathbf{G})^{\mathrm{T}}(\mathbf{E}_1+\mathbf{E}_2\mathbf{G})\right]\mathbf{P}^{-1} \end{bmatrix} < \mathbf{0}. \tag{27}$$

Let $\mathbf{X} = \mathbf{P}^{-1}, \mathbf{Y} = \mathbf{G}\mathbf{P}^{-1}$ and we get

$$\begin{bmatrix} \varepsilon\mathbf{D}\mathbf{D}^{\mathrm{T}}-\mathbf{X} & \mathbf{AX}+\mathbf{BY} \\ (\mathbf{AX}+\mathbf{BY})^{\mathrm{T}} & -\mathbf{X}+\mathbf{X}\mathbf{Q}^*\mathbf{X}+\mathbf{Y}^{\mathrm{T}}\mathbf{R}^*\mathbf{Y}+\varepsilon^{-1}(\mathbf{E}_1\mathbf{X}+\mathbf{E}_2\mathbf{Y})^{\mathrm{T}}(\mathbf{E}_1\mathbf{X}+\mathbf{E}_2\mathbf{Y}) \end{bmatrix} < \mathbf{0}. \tag{28}$$

By the Schur complementary property of matrices, (28) can be equated to

$$\begin{bmatrix} \varepsilon\mathbf{D}\mathbf{D}^{\mathrm{T}}-\mathbf{X} & \mathbf{AX}+\mathbf{BY} & \mathbf{0} \\ (\mathbf{AX}+\mathbf{BY})^{\mathrm{T}} & -\mathbf{X}+\mathbf{X}\mathbf{Q}^*\mathbf{X}+\mathbf{Y}^{\mathrm{T}}\mathbf{R}^*\mathbf{Y} & (\mathbf{E}_1\mathbf{X}+\mathbf{E}_2\mathbf{Y})^{\mathrm{T}} \\ \mathbf{0} & \mathbf{E}_1\mathbf{X}+\mathbf{E}_2\mathbf{Y} & -\varepsilon\mathbf{I} \end{bmatrix} < \mathbf{0}. \tag{29}$$

Then,

$$\begin{bmatrix} \varepsilon\mathbf{D}\mathbf{D}^{\mathrm{T}}-\mathbf{X} & \mathbf{AX}+\mathbf{BY} & \mathbf{0} \\ (\mathbf{AX}+\mathbf{BY})^{\mathrm{T}} & -\mathbf{X}+\mathbf{Y}^{\mathrm{T}}\mathbf{R}^*\mathbf{Y} & (\mathbf{E}_1\mathbf{X}+\mathbf{E}_2\mathbf{Y})^{\mathrm{T}} \\ \mathbf{0} & \mathbf{E}_1\mathbf{X}+\mathbf{E}_2\mathbf{Y} & -\varepsilon\mathbf{I} \end{bmatrix} - \begin{bmatrix} \mathbf{0} \\ \mathbf{X} \\ \mathbf{0} \end{bmatrix}\left(-\mathbf{Q}^*\right)\begin{bmatrix} \mathbf{0} \\ \mathbf{X} \\ \mathbf{0} \end{bmatrix}^{\mathrm{T}} < \mathbf{0}. \tag{30}$$

Applying the Schur complementary property of matrices, we get

$$\begin{bmatrix} \varepsilon\mathbf{D}\mathbf{D}^{\mathrm{T}}-\mathbf{X} & \mathbf{AX}+\mathbf{BY} & \mathbf{0} & \mathbf{0} \\ (\mathbf{AX}+\mathbf{BY})^{\mathrm{T}} & -\mathbf{X}+\mathbf{Y}^{\mathrm{T}}\mathbf{R}^*\mathbf{Y} & (\mathbf{E}_1\mathbf{X}+\mathbf{E}_2\mathbf{Y})^{\mathrm{T}} & \mathbf{X} \\ \mathbf{0} & \mathbf{E}_1\mathbf{X}+\mathbf{E}_2\mathbf{Y} & -\varepsilon\mathbf{I} & \mathbf{0} \\ \mathbf{0} & \mathbf{X} & \mathbf{0} & -(\mathbf{Q}^*)^{-1} \end{bmatrix} < \mathbf{0}. \tag{31}$$

Then,

$$\begin{bmatrix} \varepsilon\mathbf{D}\mathbf{D}^{\mathrm{T}}-\mathbf{X} & \mathbf{AX}+\mathbf{BY} & \mathbf{0} & \mathbf{0} \\ (\mathbf{AX}+\mathbf{BY})^{\mathrm{T}} & -\mathbf{X} & (\mathbf{E}_1\mathbf{X}+\mathbf{E}_2\mathbf{Y})^{\mathrm{T}} & \mathbf{X} \\ \mathbf{0} & \mathbf{E}_1\mathbf{X}+\mathbf{E}_2\mathbf{Y} & -\varepsilon\mathbf{I} & \mathbf{0} \\ \mathbf{0} & \mathbf{X} & \mathbf{0} & -(\mathbf{Q}^*)^{-1} \end{bmatrix} - \begin{bmatrix} \mathbf{0} \\ \mathbf{Y}^{\mathrm{T}} \\ \mathbf{0} \\ \mathbf{0} \end{bmatrix}\left(-\mathbf{R}^*\right)\begin{bmatrix} \mathbf{0} \\ \mathbf{Y}^{\mathrm{T}} \\ \mathbf{0} \\ \mathbf{0} \end{bmatrix}^{\mathrm{T}} < \mathbf{0}. \tag{32}$$

By applying the Schur complementary property of matrices again, it is found that (32) is equivalent to the constraint (i) in problem (19).

For the constraint (ii) in problem (19), it is equivalent to $\mathbf{W} > \mathbf{X}^{-1} > \mathbf{0}$ by the Schur complementary property of matrices. So, the minimization of Trace$(\mathbf{W})$ guarantees the minimization of Trace$(\mathbf{X}^{-1})$, then it is the minimization of the upper bound of system performance. Since the objective function and constraints in problem (17) are convex functions of the variables, problem (19) is a convex optimization problem so that a global minimum can be achieved. The proof is obtained by Theorem 2. □

4. Overlapping Decentralized Control Method for Discrete-Time Systems

Consider the following state-space model of a linearly continuous-time-invariant system:

$$\begin{aligned} \mathbf{S}&: \dot{Z}(t) = (\mathbf{A} + \Delta\mathbf{A})\mathbf{Z}(t) + (\mathbf{B} + \Delta\mathbf{B})\mathbf{u}(t), \\ &\mathbf{y}(t) = \mathbf{C}_y\mathbf{Z}(t), \\ \tilde{\mathbf{S}}&: \dot{\tilde{Z}}(t) = (\tilde{A} + \Delta\tilde{A})\tilde{Z}(t) + (\tilde{B} + \Delta\tilde{B})\tilde{u}(t), \\ &\tilde{y}(t) = \tilde{C}_y\tilde{Z}(t), \end{aligned} \tag{33}$$

where $\mathbf{Z}(t) \in \mathbf{R}^{\mathrm{n}}$, $\tilde{Z}(t) \in \mathbf{R}^{\tilde{\mathrm{n}}}$ represent the state vector of the system $\mathbf{S}$ and system $\tilde{\mathbf{S}}$, respectively; $\mathbf{u}(t) \in \mathbf{R}^{\mathrm{m}}$, $\tilde{u}(t) \in \mathbf{R}^{\tilde{\mathrm{m}}}$ represent the input vector of the system $\mathbf{S}$ and system $\tilde{\mathbf{S}}$, respectively; $\mathbf{y}(t) \in \mathbf{R}^{\mathrm{l}}$, $\tilde{y}(t) \in \mathbf{R}^{\mathrm{l}}$ represent the output vector of the system $\mathbf{S}$ and system $\tilde{\mathbf{S}}$, respectively; $\mathbf{A}$, $\mathbf{B}$, $\mathbf{C}_y$, $\tilde{A}$, $\tilde{B}$, and $\tilde{C}_y$ are $n \times n$, $n \times m$, $l \times n$, $\tilde{n} \times \tilde{n}$, $\tilde{n} \times \tilde{m}$, and $\tilde{l} \times \tilde{n}$ dimensional matrices, respectively. $n \le \tilde{n}$, $m \le \tilde{m}$, $l \le \tilde{l}$. Based on the inclusion principle, system $\mathbf{S}$ is extended to obtain system $\tilde{S}$, then

$$\begin{aligned} \tilde{A} &= \mathbf{VAU} + \mathbf{M}_A, \\ \tilde{B} &= \mathbf{VBQ} + \mathbf{N}_B, \\ \tilde{C}_y &= \mathbf{TC}_y\mathbf{U} + \mathbf{L}_C, \\ \Delta\tilde{A} &= \mathbf{V}\Delta\mathbf{AU}, \\ \Delta\tilde{B} &= \mathbf{V}\Delta\mathbf{BQ}, \end{aligned} \tag{34}$$

where $\mathbf{M}_A$, $\mathbf{N}_B$, $\mathbf{L}_C$ are the corresponding compensation matrices.

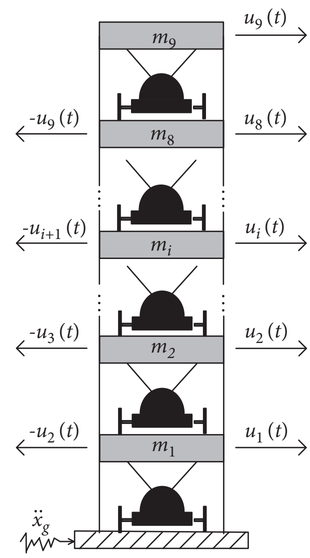

FIGURE 1: Structural model of the 9-story building.

The system $\mathbf{S}$ is extended and decoupled into L substructures after eliminating the connection blocks [32]:

$$\begin{aligned} \tilde{\mathbf{S}}_D^{(i)}&: \dot{\tilde{Z}}_i(t) = \left(\tilde{A}_{ii} + \Delta\tilde{A}_{ii}\right)\tilde{Z}_i(t) + \left(\tilde{B}_{ii} + \Delta\tilde{B}_{ii}\right)\tilde{u}_i(t), \\ &\tilde{y}_i(t) = \left(\tilde{C}_y\right)_{ii}\tilde{Z}_i(t), i = 1, 2, \ldots, L, \end{aligned} \tag{35}$$

where $\tilde{A}_{ii}$, $\tilde{B}_{ii}$ represent the known constant matrices. $\Delta\tilde{A}_{ii}$, $\Delta\tilde{B}_{ii}$ represent the unknown matrices of uncertain parameters in the model and have the following form:

$$\left[\Delta\tilde{A}_{ii} \quad \Delta\tilde{B}_{ii}\right] = \tilde{D}_i\tilde{F}_i(t)\left[\tilde{E}_{i1} \quad \tilde{E}_{i2}\right], \tag{36}$$

where $\tilde{D}_i$, $\tilde{E}_{i1}$, $\tilde{E}_{i2}$ represent the matrices of known constants with uncertain parameters. $\tilde{F}_i(t)$ represents an unknown matrix, and $\tilde{F}_i^{\mathrm{T}}(t)\tilde{F}_i(t) \le \mathbf{I}$.

Taking the sampling period $\Delta T = 0.02s$, the continuous-time system (35) is discretized, then

$$\tilde{\mathbf{S}}_\tau^{(i)}: \left\{ \dot{\tilde{Z}}_{\tau i}(k+1) = \left(\tilde{A}_{\tau ii} + \Delta\tilde{A}_{\tau ii}\right)\tilde{Z}_{\tau i}(k) + \left(\tilde{B}_{\tau ii} + \Delta\tilde{B}_{\tau ii}\right)\tilde{u}_{\tau i}(k), \tilde{y}_{\tau i}(k) = \left(\tilde{C}_y\right)_{\tau ii}\tilde{Z}_{\tau i}(k), i = 1, 2, \ldots, L. \right. \tag{37}$$

According to Theorem 2, the controller design of the discrete-time model of the subsystem is carried out to obtain the state feedback gain matrices $\tilde{G}_i$ of the subsystems, which represented the state feedback gain matrices of a block diagonal:

$$\tilde{G} = \mathrm{diag}\left\{\tilde{G}_1, \tilde{G}_2, \cdots, \tilde{G}_L\right\}. \tag{38}$$

The overlapping controller can be obtained by transforming the gain matrices $\tilde{G}$ based on the contraction principle [32]:

$$\mathbf{G} = \mathbf{Q}\tilde{\mathbf{G}}\mathbf{V}. \tag{39}$$

5. Example Simulation and Analysis

Taking the 9-story Benchmark steel structure model (as shown in Figure 1) as the simulation example, the plan and elevation of the structure can be seen in literature [33, 34]. The static coalescence method is used to reduce the order of the original finite element model, which reduces the degrees of freedom of vertical vibration and rotation and only retains nine translational freedoms of the original structure. The

Table 1: Parameters of 9-story Benchmark steel structure model.

Number of layers	1	2	3	4	5	6	7	8	9
Mass (10^5 kg)	10.1	9.89	9.89	9.89	9.89	9.89	9.89	9.89	10.7
Stiffness (10^8 N/m)	1.87	4.72	4.27	3.83	3.44	3.01	2.26	1.97	1.67

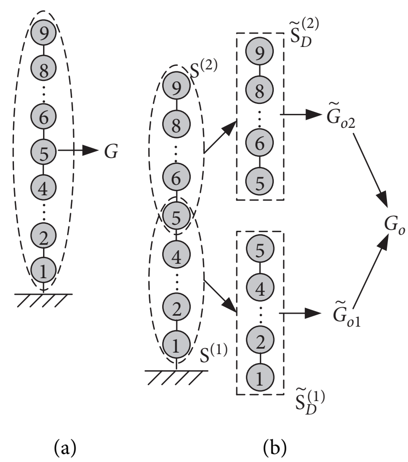

Figure 2: The design of 9-story structure controller. (a) Centralized controller. (b) Overlapping controller.

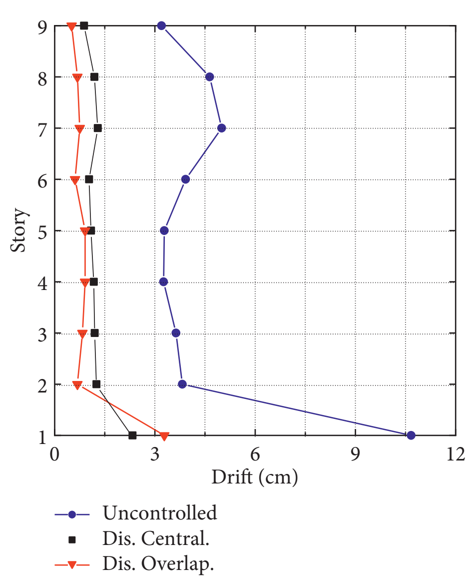

Figure 3: The peak structural interstory displacement ($\boldsymbol{\Delta M} = 0$, $\boldsymbol{\Delta C} = 0$, $\boldsymbol{\Delta K} = 0$).

corresponding parameters of the structure are listed in Table 1 [34]. The damping of the structure is Rayleigh damping, assuming the damping ratio of the first two orders of vibration is 0.02. Each layer of the structure is equipped with a drive using the interlayer drive method. The external excitation is a horizontal seismic load. The El Centro seismic wave (NS, 1940) is selected, peak acceleration is 3.0 m/s^2, duration is 30 s, and sampling step is 0.02 s.

The maximum variances that exist for the mass, damping, and stiffness of the structure are considered to be ±10%, ±15%, and ±15%, respectively. The equation of motion for uncertain parameters structural system under earthquake is shown in (1), and (2) are $\Delta\mathbf{M} = \alpha\mathbf{M}$, $\Delta\mathbf{C} = \beta\mathbf{C}$, $\Delta\mathbf{K} = \gamma\mathbf{K}$. $\mathbf{M}$, $\mathbf{C}$, $\mathbf{K}$ represent the nominal mass, damping, and stiffness matrices of the structure, respectively. The corresponding uncertain parameters in (5) can be expressed as

$$\begin{aligned}
\Delta\mathbf{A}_p &= \mathbf{D}_p\mathbf{F}_p\mathbf{E}_{p1}, \\
\Delta\mathbf{B}_p &= \mathbf{D}_p\mathbf{F}_p\mathbf{E}_{p2}, \\
\mathbf{D}_p &= \begin{bmatrix} \mathbf{0} & \mathbf{0} \\ -\mathbf{M}^{-1} & -\mathbf{M}^{-1} \end{bmatrix}_{18\times 18}, \\
\mathbf{F}_p &= \delta[\mathbf{I}]_{18\times 18} \\
\mathbf{E}_{p1} &= \begin{bmatrix} \dfrac{\beta-\alpha}{1+\alpha}\mathbf{K} & \mathbf{0} \\ \mathbf{0} & \dfrac{\gamma-\alpha}{1+\alpha}\mathbf{C} \end{bmatrix}_{18\times 18}, \\
\mathbf{E}_{p2} &= \begin{bmatrix} \mathbf{0} \\ \dfrac{\alpha}{1+\alpha}\mathbf{B}_u \end{bmatrix}_{18\times 9}.
\end{aligned} \tag{40}$$

δ is an uncertain real scalar, $|\delta| \le 1$.

For the discrete-time system of building structure with uncertain parameters, the discrete-time system state feedback overlapping decentralized guaranteed cost control method (Dis. Overlap.) and the discrete-time system state feedback centralized guaranteed cost control method (Dis.

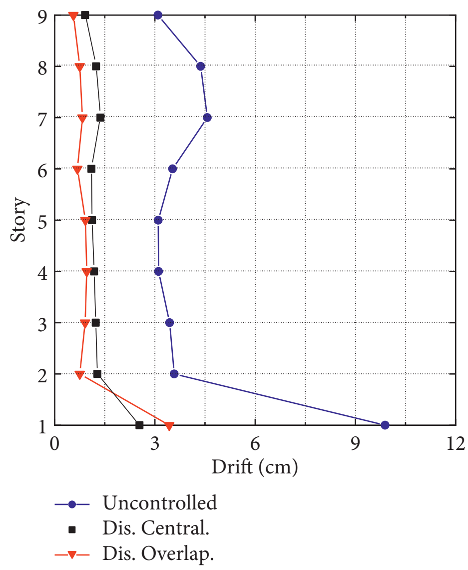

Figure 4: The peak structural interstory displacement ($\boldsymbol{\Delta M = +0.10M}$, $\boldsymbol{\Delta C = +0.15C}$, $\boldsymbol{\Delta K = +0.15K}$).

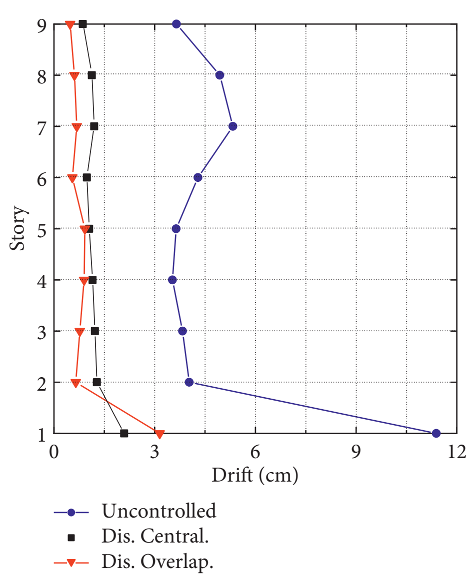

Figure 5: The peak structural interstory displacement ($\boldsymbol{\Delta M = -0.10M}$, $\boldsymbol{\Delta C = -0.15C}$, $\boldsymbol{\Delta K = -0.15K}$).

Central.) are used for numerical analysis. The design of the controller is shown in Figure 2.

According to the design steps of overlapping decentralized control method described in Section 4, the 9-story structure is overlapped and decomposed into 2 substructures, and the overlapping part is chosen as the fifth layer, then the two decoupled subsystems are $\widetilde{S}_D^{(1)} = [1, 2, \ldots, 5]$ and $\widetilde{S}_D^{(2)} = [5, 7, \ldots, 9]$. After performing discretization, the discrete-time subsystems $\widetilde{\mathbf{S}}_\tau^{(1)}$ and $\widetilde{\mathbf{S}}_\tau^{(2)}$ are obtained. The corresponding weighting matrices can be expressed as follows:

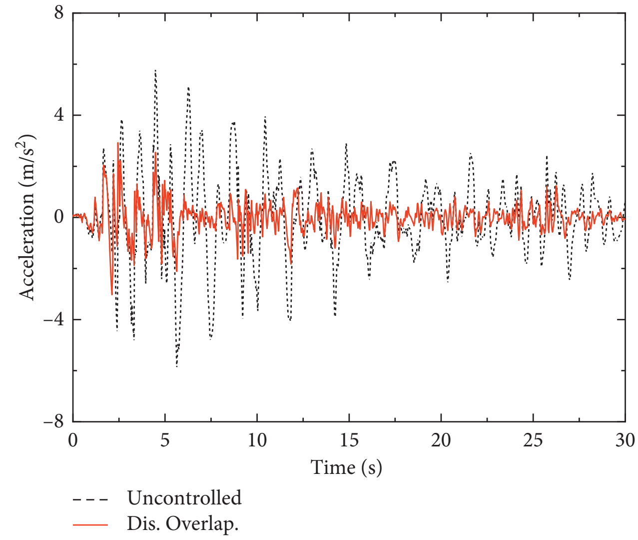

Figure 6: Acceleration time-history curves ($\boldsymbol{\Delta M = 0}$, $\boldsymbol{\Delta C = 0}$, $\boldsymbol{\Delta K = 0}$).

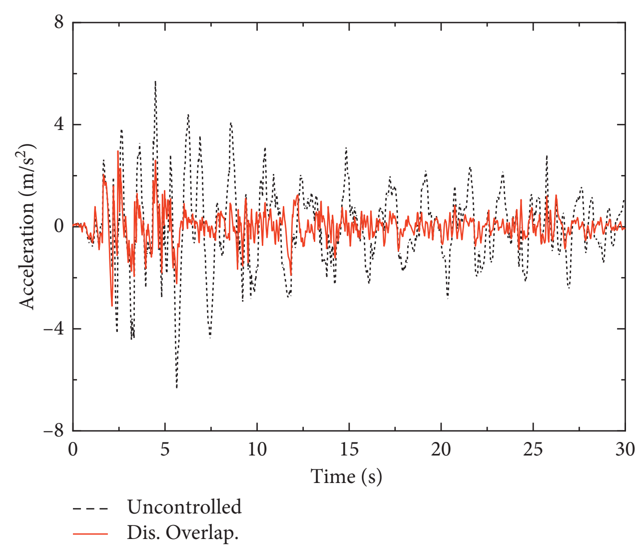

Figure 7: Acceleration time-history curves ($\boldsymbol{\Delta M = +0.10M}$, $\boldsymbol{\Delta C = +0.15C}$, $\boldsymbol{\Delta K = +0.15K}$).

$$\begin{aligned}
\widetilde{Q}_1^* &= 9.0 \times 10^4 \mathbf{I}_{10}, \\
\widetilde{R}_1^* &= 10^{-6} \mathbf{I}_5, \\
\widetilde{Q}_2^* &= 4.0 \times 10^3 \mathbf{I}_{10}, \\
\widetilde{R}_2^* &= 10^{-6} \mathbf{I}_5.
\end{aligned} \tag{41}$$

We can get $\widetilde{\varepsilon}_i$, $\widetilde{Y}_i$, $\widetilde{X}_i$, $\widetilde{W}_i$ by solving the linear matrix inequality according to Theorem 2, then the state feedback gain matrix of the subsystem can be found, which can be expressed in the form of a block diagonal matrix $\widetilde{G}_o = \operatorname{diag}[\widetilde{G}_{o1}, \widetilde{G}_{o2}]$. The gain matrices of the original system $\mathbf{G}_o = \mathbf{Q}_o \widetilde{G}_o \mathbf{V}_o$ are obtained based on shrinkage principle and linear transformation.

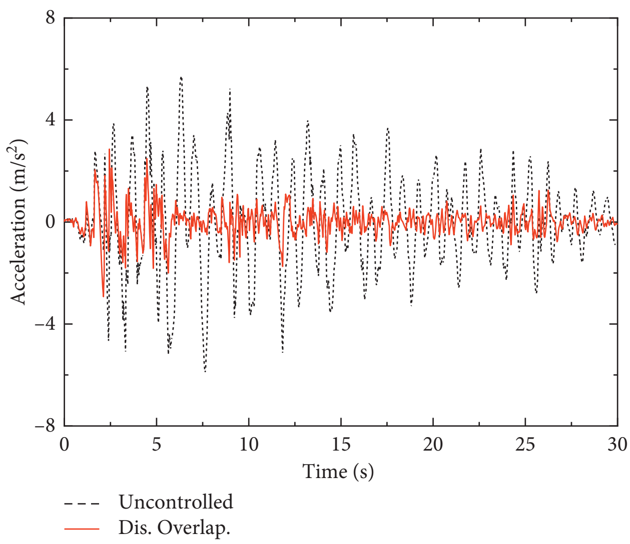

FIGURE 8: Acceleration time-history curves ($\Delta M = -0.10M$, $\Delta C = -0.15C$, $\Delta K = -0.15K$).

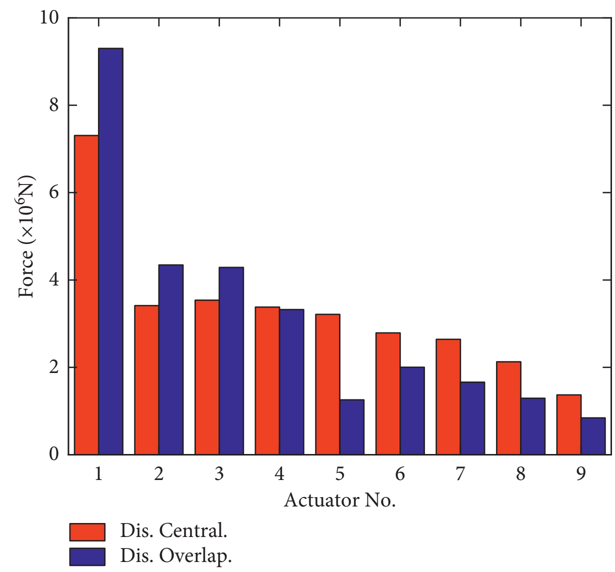

FIGURE 10: Maximum control force ($\Delta M = +0.10M$, $\Delta C = +0.15C$, $\Delta K = +0.15K$).

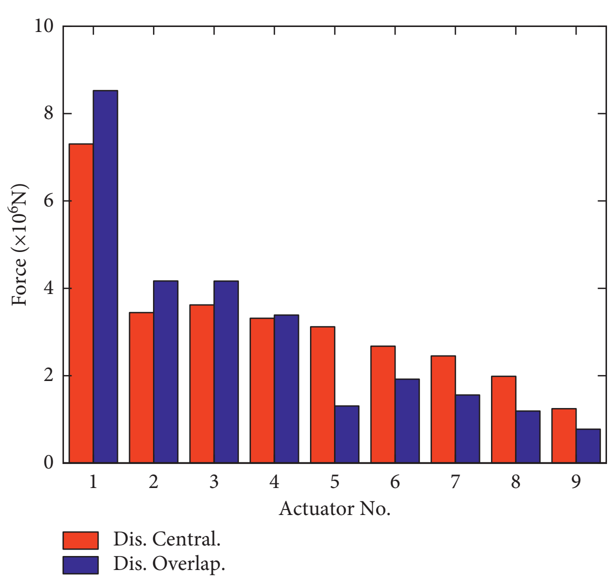

FIGURE 9: Maximum control force ($\Delta M = 0$, $\Delta C = 0$, $\Delta K = 0$).

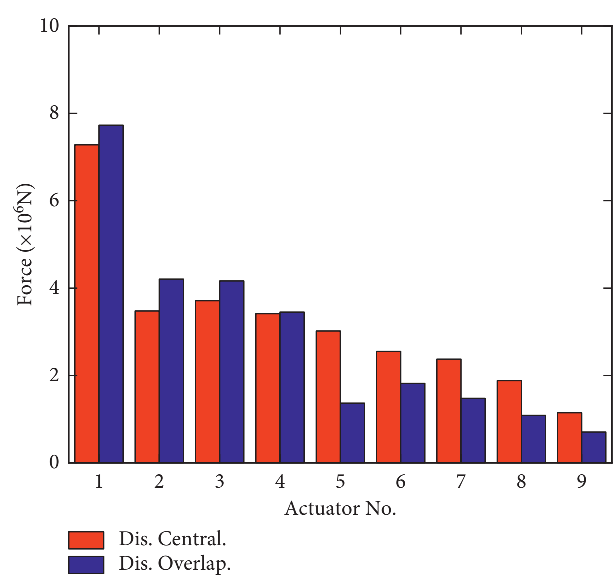

FIGURE 11: Maximum control force ($\Delta M = -0.10M$, $\Delta C = -0.15C$, $\Delta K = -0.15K$).

Figures 3–5 show the comparison of the peak interstory displacement responses of the structure with uncertain parameters using uncontrolled (Uncontrolled), discrete-time overlapping decentralized guaranteed cost control method (Dis. Overlap.) and discrete-time centralized guaranteed cost control method (Dis. Central.).

It can be seen from Figures 3–5 as follows: (1) when the errors of structural parameters are $\Delta M = 0$, $\Delta C = 0$, and $\Delta K = 0$, the interstory displacement control effect of discrete-time centralized guaranteed cost control method (Dis. Central.) is 64.11% ~ 78.16% with an average control rate of 70.89%; the interstory displacement control effect of discrete-time overlapping decentralized guaranteed cost control method (Dis. Overlap.) is 69.26% ~ 85.34% with an average control rate of 79.09%. (2) When the errors of structural parameters are $\Delta M = +0.10\,M$, $\Delta C = +0.15\,C$, and $\Delta K = +0.15\,K$, the interstory displacement control effect of discrete-time centralized guaranteed cost control method (Dis. Central.) is 62.06% ~ 74.32% with an average control rate of 67.75%; the interstory displacement control effect of discrete-time overlapping decentralized guaranteed cost control method (Dis. Overlap.) is 65.32% ~ 82.84% with an average control rate of 76.07%. (3) When the errors of structural parameters are $\Delta M = -0.10\,M$, $\Delta C = -0.15\,C$, and $\Delta K = -0.15\,K$, the interstory displacement control effect of discrete-time centralized guaranteed cost control method (Dis. Central.) is 67.42% ~ 81.65% with an average control rate of 73.87%; the interstory displacement control effect of discrete-time overlapping decentralized guaranteed cost control method (Dis. Overlap.) is 72.34% ~ 87.65% with an average control rate of 81.58%. From the above data, it can be seen that the proposed control method can achieve good control effects under the existence of uncertainty in structural parameters, and the average control rate of interstory displacement under each working condition is better than the centralized control strategy. The effectiveness and applicability of this method are illustrated.

Figures 6–8 show the comparison of the acceleration time-history curves of the structural top floor with uncertain parameters under uncontrolled and discrete-time overlapping decentralized guaranteed cost control method (Dis. Overlap.). It can be seen from the figure that the proposed decentralized control method can effectively reduce the acceleration response of the structure when the structural parameters are uncertain.

Figures 9 to 11 show the comparison of the maximum control force of the structure with uncertain parameters using the discrete-time overlapping decentralized guaranteed cost control method (Dis. Overlap.) and discrete-time centralized guaranteed cost control method (Dis. Central.). It can be seen from the figure that the output values required by the two control methods are within the range of the controller. Specifically, except for the overlapping layers, the control force required for each layer of substructure 1 is slightly greater than that of the centralized control method, and the control force required for each layer of substructure 2 is less than that of the centralized control method, in the case of comparable control effects. The reasons are as follows: (1) the overlapping decentralized guaranteed cost control method divides the original structure into two substructures which reduces the dimensionality of system. (2) Each substructure controller in the overlapping decentralized control strategy is controlled independently and works in parallel. The overlapping layer acts as a connecting layer between two substructures, and the control force is influenced by both substructures. (3) Due to the existence of overlapping layers, substructure 1 and substructure 2 are similar to the relationship between the upper and lower floors. Therefore, the control force of substructure 1 increases while the control force required for substructure 2 decreases, while the control effect is guaranteed to be constant.

6. Conclusions

This paper combines the overlapping decentralized control strategy and the guaranteed cost control algorithm and then proposes an overlapping decentralized guaranteed cost control method for discrete-time systems. The proposed method is first studied numerically with a nine-story parameters uncertainty building example. The following conclusions can be drawn from the present study:

(1) The discrete-time overlapping decentralized guaranteed cost control algorithm based on state feedback proposed can achieve satisfactory control results under the uncertainty of the controlled structural parameters. It shows that the method is suitable for solving the vibration control problem of building structural systems with uncertain parameters.

(2) The overlapping decentralized control strategy has a better average control rate of interlayer displacement compared with the centralized control strategy under the condition of comparable controller output, which illustrates the effectiveness and feasibility of the proposed method.

(3) The overlapping decentralized control method realizes the dimensionality reduction of large systems. In low-dimensional systems, the transmission speed of signals is rapid, the data processing is efficient, and the computational cost is low, which provides an effective idea for solving the vibration control problems of complex systems.

Data Availability

The data used to support the study are available from the corresponding authors upon request.

Conflicts of Interest

The authors declare that there are no conflicts of interest regarding the publication of this paper.

Acknowledgments

This study was financially supported by the Natural Science Research Project of Higher Education Institutions in Anhui Province (KJ2019A0748, KJ2019A0747, and KJ2020A0490), the Doctoral Startup Foundation of Anhui Jianzhu University (2018QD28, 2017QD05, 2020QDZ07, and 2020QDZ38), the Anhui Provincial Natural Science Foundation (Grant Nos. 2008085QE245 and 2108085QA41), the Project of Science and Technology Plan of Department of Housing and Urban-Rural Development of Anhui Province (2019YF-029, 2020-YF20, and 2021-YF22), and the School-Enterprise Cooperative Development Project of Anhui Jianzhu University (HYB20190137).

References

[1] J. Tao and O. Mercan, “A study on a benchmark control problem for real-time hybrid simulation with a tracking error-based adaptive compensator combined with a supplementary proportional-integral-derivative controller,” *Mechanical Systems and Signal Processing*, vol. 134, Article ID 106346, 2019.

[2] C. E. Silva, D. Gomez, A. Maghareh, S. J. Dyke, and B. F. Spencer Jr, “Benchmark control problem for real-time hybrid simulation,” *Mechanical Systems and Signal Processing*, vol. 135, Article ID 106381, 2020.

[3] Ö. Şahin, N. G. Adar, M. Kemerli et al., “A comparative evaluation of semi-active control algorithms for real-time seismic protection of buildings via magnetorheological fluid dampers,” *Journal of Building Engineering*, vol. 42, Article ID 102795, 2021.

[4] B. D. Winter and R. A. Swartz, "Wireless structural control using stochastic bandwidth allocation and dynamic state estimation with measurement fusion," *Structural Control and Health Monitoring*, vol. 25, no. 2, Article ID e2104, 2018.

[5] M. C. Vásquez and R. Katebi, "New constrained predictive PID controller for packet dropouts in wireless networked control systems," *IFAC-PapersOnLine*, vol. 51, no. 4, pp. 811–816, 2018.

[6] H. Su, H. Zhang, X. Liang, and C. Liu, "Decentralized event-triggered online adaptive control of unknown large-scale systems over wireless communication networks," *IEEE Transactions on Neural Networks and Learning Systems*, vol. 31, no. 11, pp. 4907–4919, 2020.

[7] S. Shi, Z. Shi, Z. Fei, and Z. Liu, "Finite-time output feedback control for discrete-time switched linear systems with mode-dependent persistent dwell-time," *Journal of the Franklin Institute*, vol. 355, no. 13, pp. 5560–5575, 2018.

[8] S. Paul, W. Yu, and X. Li, "Discrete-time sliding mode for building structure bidirectional active vibration control," *Transactions of the Institute of Measurement and Control*, vol. 41, no. 2, pp. 433–446, 2019.

[9] M. Kemerli, Ö. Şahin, İ. Yazıcı, N. Çağlar, and T. Engin, "Comparison of discrete-time sliding mode control algorithms for seismic control of buildings with magneto-rheological fluid dampers," *Journal of Vibration and Control*, Article ID 10775463211070062, 2022.

[10] O. Demir and H. Özbay, "Static output feedback stabilization of discrete time linear time invariant systems based on approximate dynamic programming," *Transactions of the Institute of Measurement and Control*, vol. 42, no. 16, pp. 3168–3182, 2020.

[11] F. Gómez and W. Yu, "Discrete-time tri-directional active control of building structures," *Engineering Structures*, vol. 243, Article ID 112689, 2021.

[12] M. Z. Doghmane, M. Kidouche, S. Eladj, and B. Belahcene, "Design of optimal decentralized controller using overlapping decomposition for smart building system," *Artificial Intelligence and Renewables Towards an Energy Transition*, vol. 174, pp. 155–167, 2020.

[13] X. F. Kang, P. P. Zhang, Y. Y. Zhang et al., "Decentralized control strategies of adjacent building structures vibration under earthquake excitation," *Mathematical Problems in Engineering*, vol. 2021, Article ID 9964019, 14 pages, 2021.

[14] X. F. Kang, J. Wu, Y. Y. Zhang et al., "Overlapping decentralized control strategies of building structures' vibration with time delay based on H∞ control algorithms under seismic excitation," *Shock and Vibration*, vol. 2021, Article ID 9115938, 12 pages, 2021.

[15] A. Warsewa, J. L. Wagner, M. Böhm, O. Sawodny, and C. Tarín, "Decentralized LQG control for adaptive high-rise structures," *IFAC-PapersOnLine*, vol. 53, no. 2, pp. 9131–9137, 2020.

[16] G. Liu, W. Jiang, Q. Yang, Q. Wang, and S. S. Law, "Decentralized state feedback control of linear time-invariant system with free-interface substructures," *Structures*, vol. 34, pp. 4908–4919, 2021.

[17] H. N. Fadhilah, G. Zhai, D. Adzkiya, and E. Apriliani, "H∞ state feedback for linear systems with decentralized control inputs," *Science and Nature*, vol. 2, no. 4, pp. 219–231, 2019.

[18] F. Palacios-Quiñonero, J. Rubió-Masségú, J. M. Rossell, and H. R. Karimi, "An effective computational design strategy for H∞ vibration control of large structures with information constraints," *Engineering Structures*, vol. 171, pp. 298–308, 2018.

[19] A. Aboudonia, A. Martinelli, and J. Lygeros, "Passivity-based decentralized control for discrete-time large-scale systems," in *Proceedings of the 2021 American Control Conference (ACC)*, pp. 2037–2042, Orleans, LA, USA, 2021.

[20] Y. Zhu and E. Fridman, "Predictor methods for decentralized control of large-scale systems with input delays," *Automatica*, vol. 116, Article ID 108903, 2020.

[21] A. Warsewa, M. Böhm, P. Rapp, O. Sawodny, and C. Tarın, "Decentralized and distributed observer design for large-scale structures using dynamic condensation," in *Proceedings of the 2019 IEEE 15th International Conference on Automation Science and Engineering (CASE)*, pp. 1256–1262, 2019.

[22] Q. H. Xu, X. Z. Zhen, X. Ruan et al., "The research of the overlapping decentralized guaranteed cost hybrid control method for adjacent buildings with uncertain parameters," *Mathematical Problems in Engineering*, vol. 2022, Article ID 1143374, 14 pages, 2022.

[23] L. Zhang, Y. Xue, X. Wang, and X. Zhang, "Guaranteed cost control for a class of nonlinear discrete time-delay systems," *IEEE Access*, vol. 7, Article ID 130067, 2019.

[24] L. Chen, R. Wu, L. Yuan, L. Yin, Y. Q. Chen, and S. Xu, "Guaranteed cost control of fractional-order linear uncertain systems with time-varying delay," *Optimal Control Applications and Methods*, vol. 42, no. 4, pp. 1102–1118, 2021.

[25] F. Qi, Y. Chai, L. P. Chen, and G. A. Tenreiro Machado, "Delay-dependent and order-dependent guaranteed cost control for uncertain fractional-order delayed linear systems," *Mathematics*, vol. 9, no. 1, 2020.

[26] C. J. Chen, Z. H. Li, J. Teng, and Y. Wang, "Influence analysis of a Higher-Order CSI effect on AMD systems and its Time-Varying delay compensation using a guaranteed cost control algorithm," *Applied Sciences*, vol. 7, no. 4, 2017.

[27] Z. H. Li, C. J. Chen, J. Teng, J. K. Dong, and B. C. Lin, "A state feedback controller based on GCC algorithm against wind-induced motion for high-rise buildings with parametric uncertainties," *Shock and Vibration*, vol. 2019, Article ID 3678258, 14 pages, 2019.

[28] X. X. Feng, J. L. Wu, and Y. Q. Zhang, "Time response of structure with interval and random parameters using a new hybrid uncertain analysis method," *Applied Mathematical Modelling*, vol. 64, pp. 426–452, 2018.

[29] S. J. Kim and J. W. Choi, "Parametric uncertainty in controlling the vibration of a building," in *Proceedings of the 39th SICE Annual Conference*, pp. 107–112, Iizuka, Japan, July 2000.

[30] L. Yu, G. D. Chen, and J. Chu, "Optimal guaranteed cost control of linear uncertain system: an LMI approach," *Control Theory & Applications*, vol. 17, no. 3, pp. 423–428, 2000.

[31] L. Yu, *Robust Control, Linear Matrix Inequality Approach*, Tsinghua University Press, Beijing, 2002.

[32] F. Palacios-Quiñonero, J. M. Rossell, and H. R. Karimi, "Semi-decentralized strategies in structural vibration control," *Modeling Identification and Control*, vol. 32, no. 2, pp. 57–77, 2011.

[33] Y. Ohtori, R. E. Christenson, B. F. Spencer Jr, and S. J. Dyke, "Benchmark control problems for seismically excited nonlinear buildings," *Journal of Engineering Mechanics*, vol. 130, no. 4, pp. 366–385, 2004.

[34] P. Tan, Z. D. Pan, and F. L. Zhou, "Theoretical investigation and numerical analysis of overlapping decentralized control for complex structure," *Journal of Building Structures*, vol. 39, no. 1, pp. 69–77, 2018.